Chapter 4

Results and Discussion

In this chapter, I present chlorine K-edge Near-Edge X-Ray Absorption Fine Structure (NEXAFS) spectra for some selected small molecules of chlorine compound, including, dichloromethane (CH_2Cl_2), trichloromethane($CHCl_3$), tetrachloromethane (CCl_4) and trichlorofluoromethane (CCl_3F). Dichloromethane is useful as a solvent for many chemical processes. It is widely used as a paint stripper and a degreaser. In the food industry, dichloromethane has been used to decaffeinate coffee and tea as well as to prepare extracts of hops and other flavorings [24]. Moreover, its volatility has led to its use as an aerosol spray propellant and as a blowing agent for polyurethane foams. Concerns about its health effects, however, have led to a search for alternatives in many of these applications. The major use of trichloromethane or chloroform today is in the production of the chlorodifluoromethane (R-22), a major precursor to tetrafluoroethylene. R-22 is then converted into tetrafluoroethylene, the main precursor to Teflon. Chloroform is a common solvent in the laboratory because it is relatively unreactive, miscible with most organic liquids, and conveniently volatile. Chloroform is also used as a solvent in the pharmaceutical industry and for producing dyes and pesticides. Chloroform was once a widely-used anesthetic. Its vapor depresses the central nervous system of a patient, allowing a doctor to perform various otherwise painful procedures. Unfortunately, chloroform is as not safe an agent as ether, especially when administered by an untrained practitioner. This led to many deaths from the use of chloroform that might have been preventable [25].

Tetrachloromethane (CCl_4) is widely used as a dry cleaning solvent, as a refrigerant, and in lava lamps [26]. Tetrachloromethane is also one of the most potent hepatotoxins (toxic to the liver), and is widely used in scientific research to evaluate hepatoprotective agents [27]. For trichlorofluoromethane CCl_3F, it was the first widely used refrigerant because of its high boiling point (compared to most refrigerants). Because of the high chlorine content and the ease with which the chlorine atoms can be displaced when the molecule is subject to ultraviolet light, trichlorofluoromethane has the highest ozone depletion potential of any refrigerant, production was ended in January 1, 1996 [27].

Table 4.1 Some properties of the chlorine compound samples

Samples		Melting point at 1 atm	Boiling point at 1 atm
Trichloromonofluoromethane or freon-11 or CFC-11	CCl_3F	-110 °C	24 °C
Dichloromethane or freon-30	CH_2Cl_2	-97 °C	40°C
Trichloromethane or chloroform or freon-20	$CHCl_3$	-64 °C	61°C
Carbon tetrachloride or freon-10	CCl_4	-23°C	77°C

Table 4.2 Molecular model of the chlorine compound samples

CCl_3F	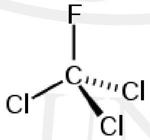	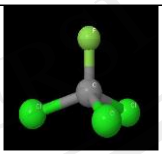
$CHCl_3$	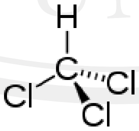	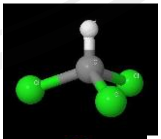
CCl_4	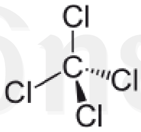	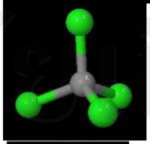
CH_2Cl_2	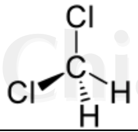	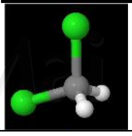

X-ray absorption in fluorescent mode was measured the samples in solid and liquid at one atmosphere and was measured in ion-yield mode for gas phases. x-ray absorption experiment on solid and liquid phase samples at one atmosphere using the endstation described in section 3.2.2, while the experiments on gas phase was performed on the gas cell described in section 3.3.

4.1 Data processing with ATHENA

ATHENA is an interactive graphical utility for processing XAFS data primarily for EXAFS. We use some features of ATHENA only to subtract background and normalize the edge step. ATHENA expects data of one of a few types. Column data in which the columns represent such things as the energy grid and the scalars measured during the experiment are the most common sort of data that most people use import into ATHENA. ATHENA's column selection dialog is used to convert the raw scalars into absorption data. For background subtraction, a smooth pre-edge background was obtained by fitting a first-order polynomial to the pre-edge region and subtracting this straight line from the entire spectrum.

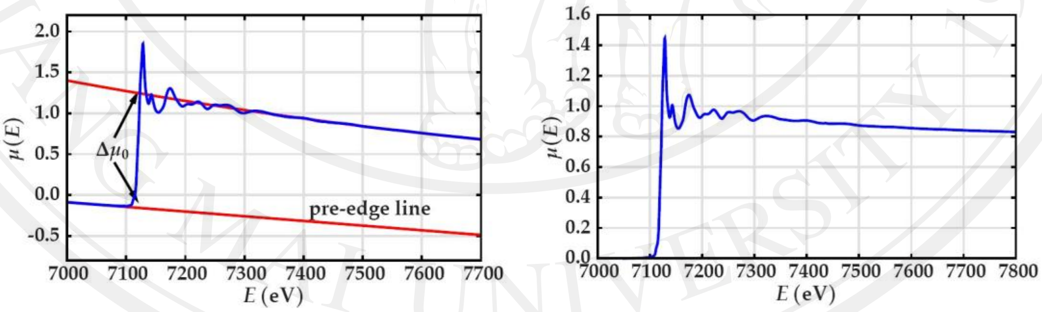

Figure 4.1: Absorption spectra with pre and post lines (Left) and normalized absorption spectra data (Right) [28].

In the normalization process we wish to scale the data so that the edge jump is set to one. Normalization of the spectra was accomplished by performing a first-order polynomial fit to data in the pre-edge region, doing a similar post-edge fit and calculating the difference between them at the edge energy, as shown in Figure 4.1 [28]. This normalization allows for comparative analysis of spectral feature in the near edge region, where absorption intensity is depend on Cl specification. Raw data is typically measured in several scans. These scans can also be merged together to give better statistics.

4.2 NEXAFS Spectra of some Cl Compounds

The Cl K-edge NEXAFS spectra for trichlorofluoromethane CCl_3F, tetrachloromethane CCl_4, trichloromethane $CHCl_3$, and dichloromethane CH_2Cl_2 in liquid, solid and gas phases were measured using the endstation and the gas absorption cell described in Chapter 3. Normally, all samples are in liquid phase with high evaporation rate at the room temperature. To reduce the evaporation rate and to freeze the sample, I use the dry-ice and liquid nitrogen to remain the each sample in liquid phase and freeze them to solid phase, as shown in Table 4.3.

Table 4.3 Methods remain and freeze sample to liquid and solid phases.

Compound (melting point, boiling point °C)	Liquid phase agent	Solid phase freezing agent
CCl_3F (-110 °C, 24 °C)	Dry-ice	Liquid Nitrogen
CCl_4 (-23 °C, 77 °C)	-	Dry-ice
$CHCl_3$ (-64 °C, 61 °C)	-	Liquid Nitrogen
CH_2Cl_2 (-97 °C, 40 °C)	Dry-ice	Liquid Nitrogen

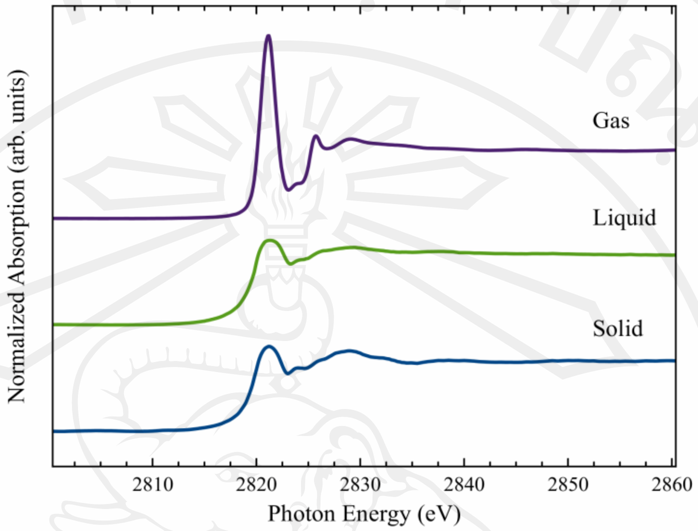

Figure 4.2: Cl K-edge NEXAFS spectra for CCl_3F molecule.

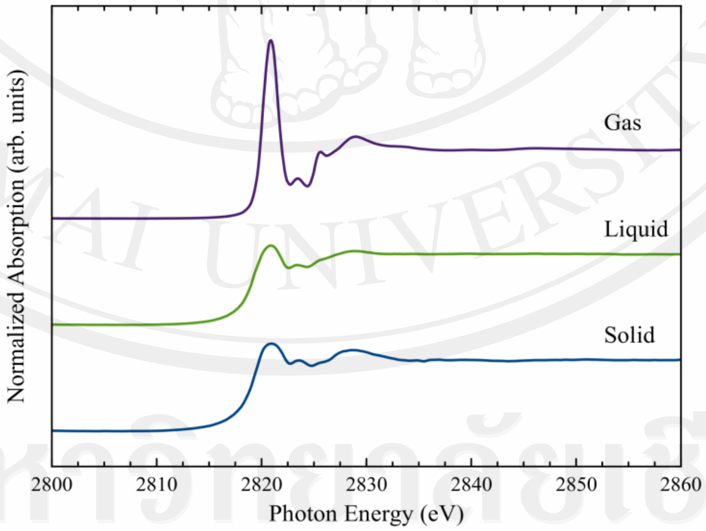

Figure 4.3: Cl K-edge NEXAFS spectra for CCl_4 molecule.

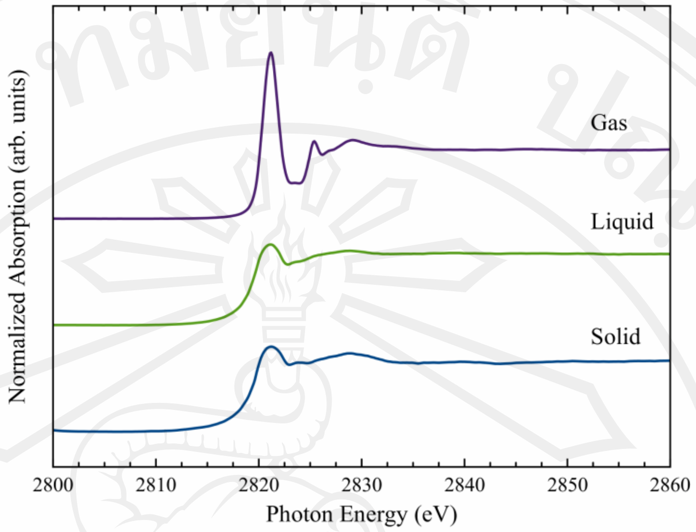

Figure 4.4: Cl K-edge NEXAFS spectra for $CHCl_3$ molecule.

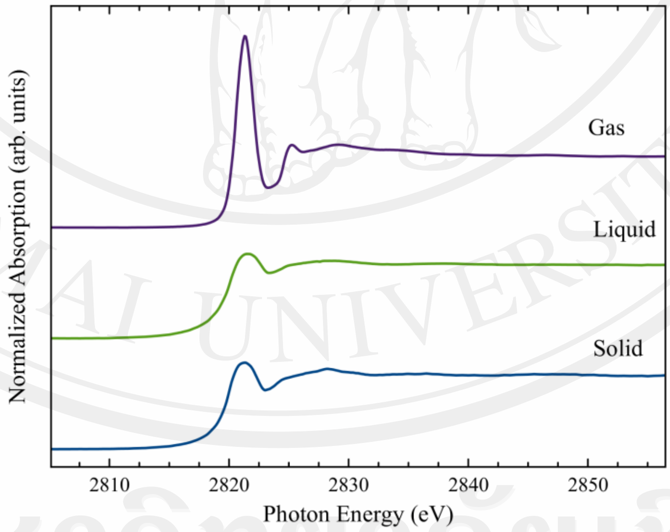

Figure 4.5: Cl K-edge NEXAFS spectra for CH_2Cl_2 molecule.

The measured NEXAFS spectra for Cl compounds in difference phases are shown in Figure 4.2 - Figure 4.5. The peak position of the spectra for different phase of each samples are not significantly different, but their shapes obviously reflect the structure depending upon their phase. There are fewer structural features on liquid spectra than for solid due to differences in the order of molecular structure between the bulk of liquid and solid. Data were collected between 2800 and 2900 eV, at intervals of 0.2 eV around the absorption edge and at the intervals of 0.5 eV before and after the edge region.

The Cl K-edge NEXAFS spectra for dichloromethane (CH_2Cl_2), trichloromethane($CHCl_3$), tetrachloromethane(CCl_4) and trichlorofluoromethane (CCl_3F) in gas, liquid and solid phases were shown in Figure 4.6 – Figure 4.8, respectively.

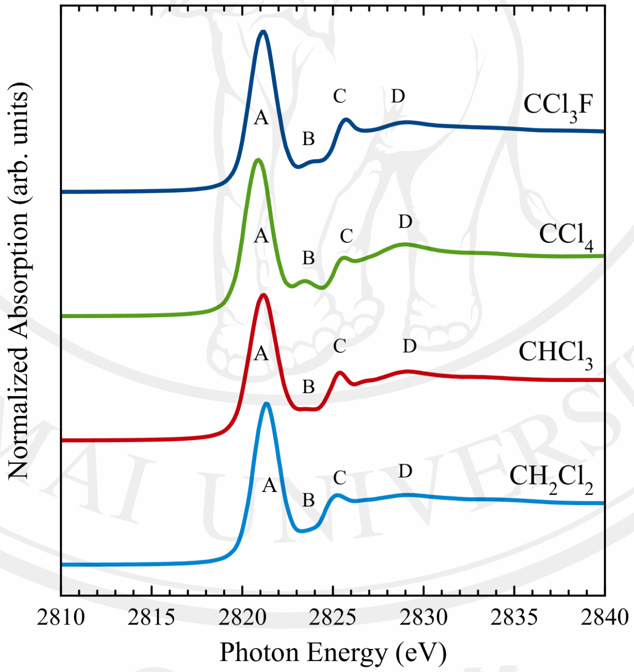

Figure 4.6: Cl K-edge NEXAFS spectra for CH_2Cl_2 , $CHCl_3$, CCl_4 , CCl_3F in gas phase.

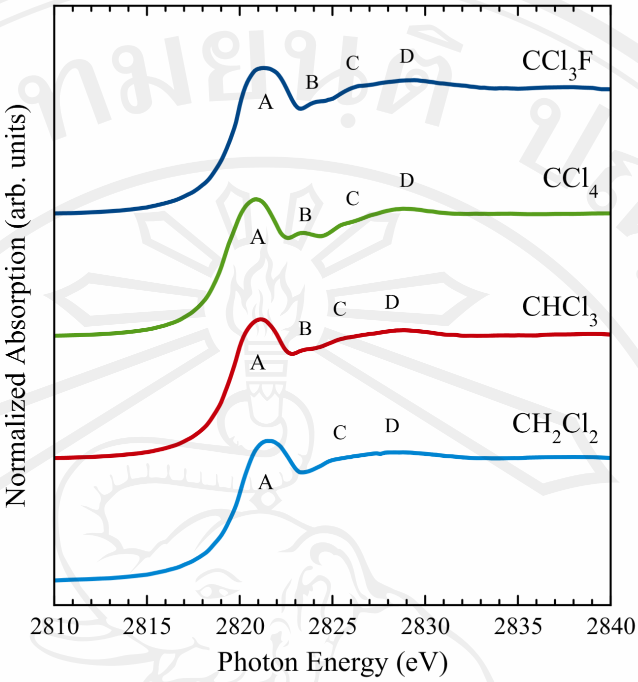

Figure 4.7: Cl K-edge NEXAFS spectra for CH_2Cl_2, $CHCl_3$, CCl_4, CCl_3F in liquid phase.

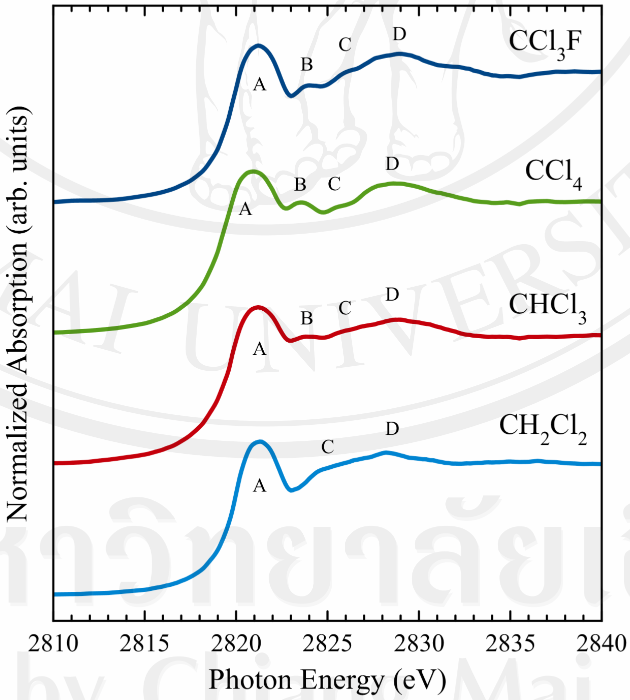

Figure 4.8: Cl K-edge NEXAFS spectra for CH_2Cl_2, $CHCl_3$, CCl_4, CCl_3F in solid phase.

The figures show that the Cl K-edge of samples remain the same for all four compounds, showing three peaks in the pre-edge region (A, B and C) and a multiple-scattering resonance region (D) above the rising edge. Going from the gas phase to the solid phase the peak D in NEXAFS spectrum is strongly modified. The peak D in the gas phase is only scattering from the nearest neighboring atoms. In solid phase, however, the scattering from atoms beyond the first neighbors of condensed system small humps appearing on both energy side of the peak D in the Cl compound spectrum, as seen in Figure 4.9. Thus, the presence of the solid phase can be easily probed by the structures of the peak D in the Cl K-edge NEXAFS spectra.

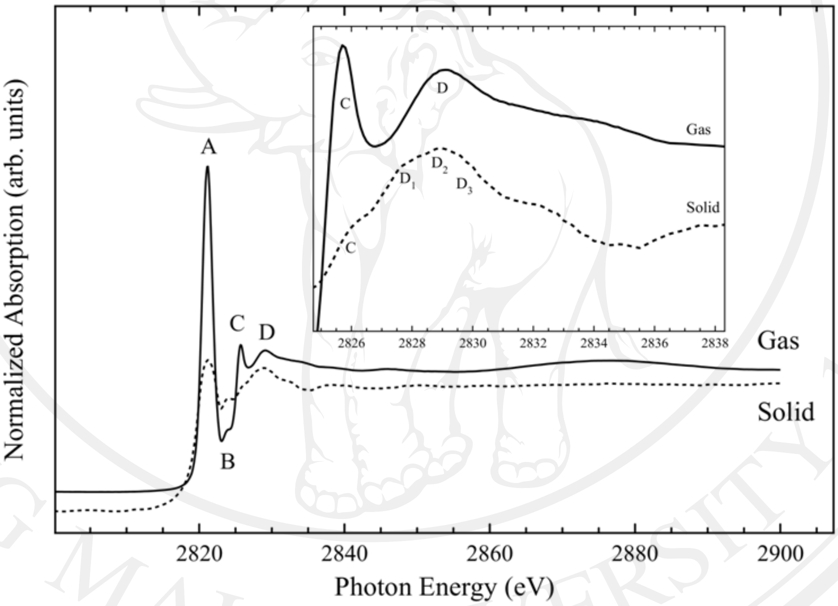

Figure 4.9: Cl K-edge NEXAFS spectra of CCl_3F in the solid and gas phase.

4.3 Deconvolution of Cl K-edge spectra

The pre-edge peaks and multiple-scattering resonance peak of the Cl K-edge NEXAFS spectra for the samples in gas phase were fit with MagicPlot Pro 2.0.1. The peaks are fit to Lorentzian shape. The number of peaks to fit into the per-edge and peak under edge regions ware determined by the number of features in the second derivative. Deconvolution that result from fitting of the pre-edge region of CCl_3F, CCl_4, $CHCl_3$, CH_2Cl_2 are shown in Figure 4.10- Figure 4.13.

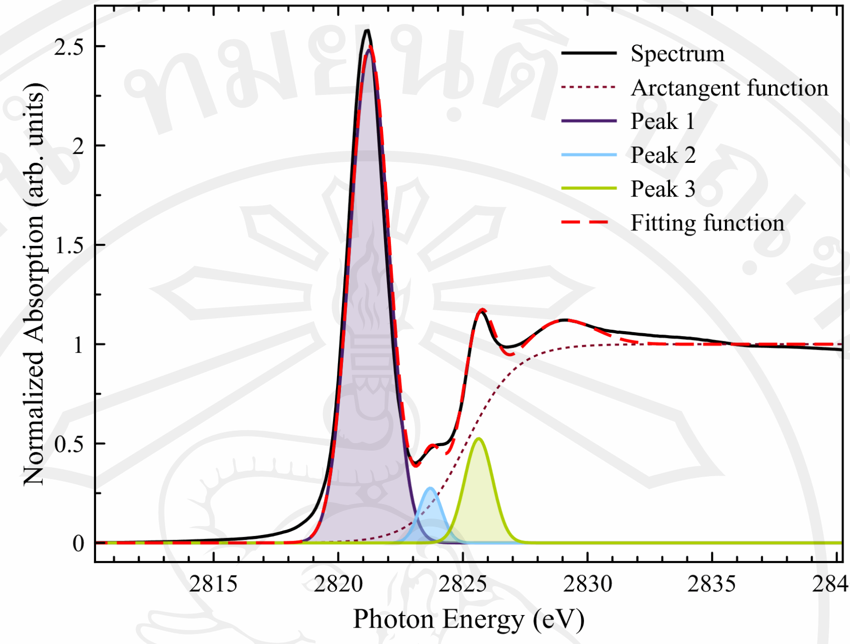

Figure 4.10: Pre-edge peak region of normalized Cl K-edge spectra of CCl_3F. Deconvolution of XANES spectra made using MagicPlot Pro 2.0.1 is shown under the data.

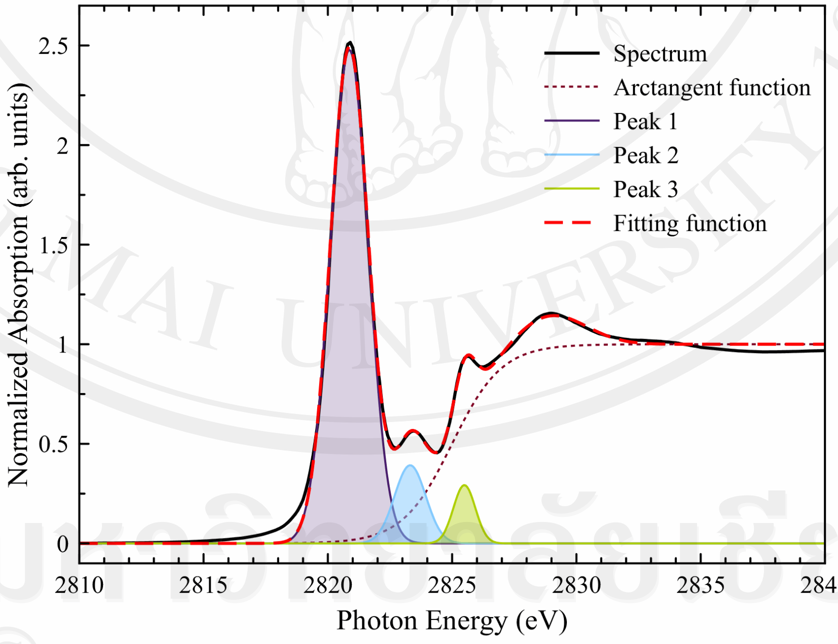

Figure 4.11: Pre-edge peak region of normalized Cl K-edge spectra of CCl_4. Deconvolution of XANES spectra made using MagicPlot Pro 2.0.1 is shown under the data.

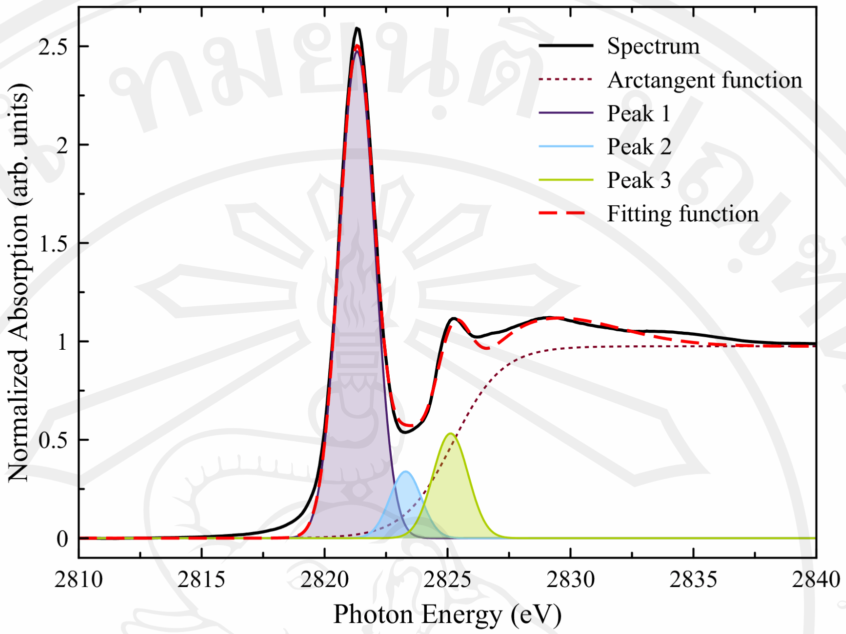

Figure 4.12: Pre-edge peak region of normalized Cl K-edge spectra of CH_2Cl_2. Deconvolution of XANES spectra made using MagicPlot Pro 2.0.1 is shown under the data.

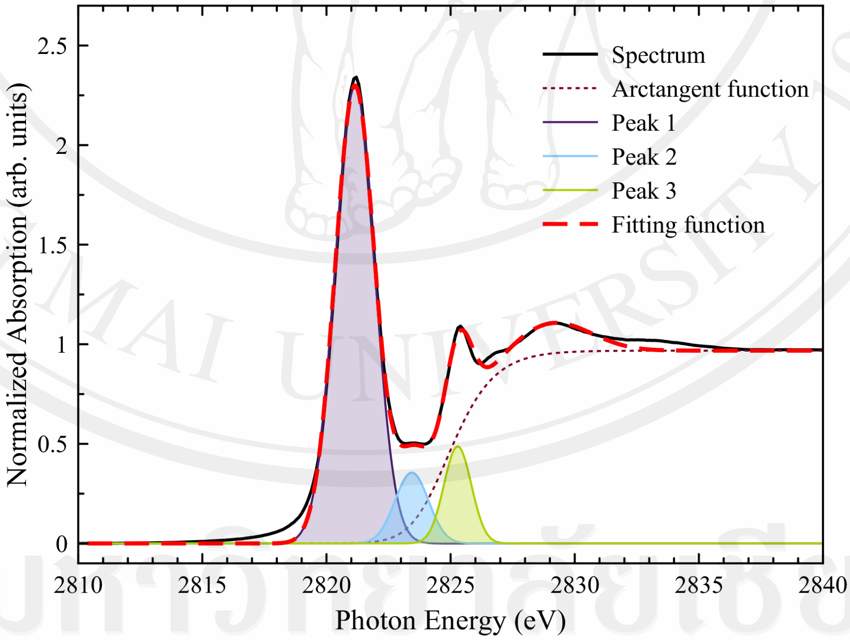

Figure 4.13: Pre-edge peak region of normalized Cl K-edge spectra of $CHCl_3$. Deconvolution of XANES spectra made using MagicPlot Pro 2.0.1 is shown under the data.

Values for energy, full width at half maximum (FWHM) and intensities of the pre-edge peaks are given in Table 4.3. For example, the second derivative and fitting of the pre-edge peak region of CCl_3F indicate that there are three pre-edge features, appearing as a shoulder on the rising edge. The energy of the first feature is 2821.2 eV. The intensity of this pre-edge peak is 4.881, based on the area measurements. The second, fit at 2823.7eV, has a peak intensity of 0.313. The third peak, at a fit energy of 2825.6, has a peak intensity of 0.742.

Table 4.4. Pre-edge and rising edge inflection Fit of Cl K-Edges of Chlorine compounds.

compound	Edge inflection (eV)	Pre-edge peak			
		Energy (eV)	amplitude	FWHM	Area
CCl_3F	2825.1	2821.2	2.481	0.924	4.881
		2823.7	0.276	0.533	0.313
		2825.6	0.525	0.664	0.742
CCl_4	2825.0	2820.9	2.479	0.898	4.739
		2823.3	0.393	0.742	0.620
		2825.5	0.293	0.521	0.325
$CHCl_3$	2824.9	2821.1	2.297	0.936	4.576
		2823.4	0.356	0.792	0.600
		2825.3	0.487	0.649	0.673
CH_2Cl_2	2824.5	2821.3	2.420	0.843	4.344
		2823.3	0.183	0.590	0.230
		2825.1	0.443	0.788	0.743

It is interesting to note that three pre-edge peaks are seen in all of the molecules, differing less than the ±0.4 eV for the spectra. It is reported in [29] that the main absorption peak results from bound excited states within molecule space.

Consider C-Cl boning, the valence orbitals are C [two 2s- and two 2p-orbitals], Cl [3s- and three 3p-orbitals]. However, carbon will be formed sp^3 hybrid orbitals by One 2s and three 2p atomic orbitals blend. The more electronegative atom is Cl, so we expect the 3s- and 3p-orbitals of Cl to be lower in energy than the sp^3 hybrid orbital of C. The covalent bond of C–Cl is formed from the overlap of the C $2sp^3$-orbital and the Cl $3p_z$-orbital. (The z-axis is customarily chosen to be the bond axis.) The correlation diagram shows the resulting σ-bonding orbital and σ*-antibonding orbital. The electronic configuration of Cl in molecule is $(Cl\ 1s)^2\ (Cl\ 2s)^2$

(Cl 2p)$^6\sigma^2$(Cl 3p$_x$)^2 (Cl 3p$_y$)^2 (σ^*)^0. The lowest unoccupied molecular orbitals are (σ^*)^0 (Cl 3d)^0, as shown in Fig. 4.14.

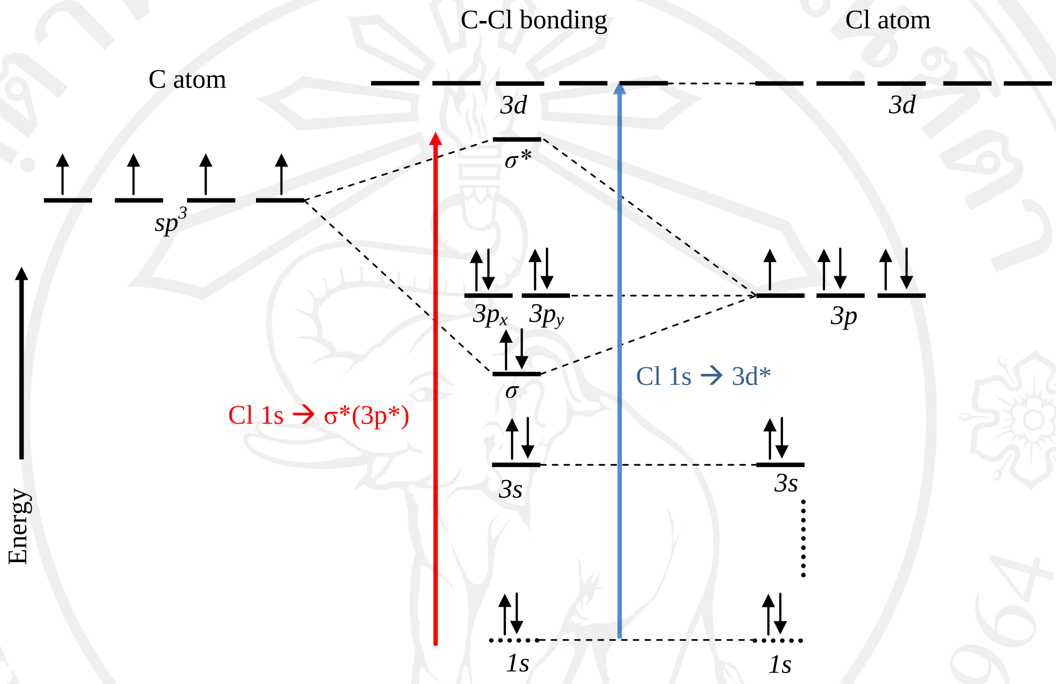

Figure 4.14: Diagram of Molecular orbital of C-Cl bonding.

The correlation diagram shows the resulting σ-bonding orbital and σ*-antibonding orbital. As seen in diagram, there are two main bound excited states of Cl compound. Accordingly, the lower energy peak (A) corresponds to a Cl 1s → σ*(3p*) transition. The higher energy peak (C) is characteristic of Cl 1s → 3d* transition.

The components of the fits of higher energy peak (C) in pre-edge region and multiple-scattering resonance (peak D) of CCl_3F, CCl_4, $CHCl_3$ and CH_2Cl_2 are shown in Figure 4.15. The peak energies and areas for these molecules are given in Table 4.5.

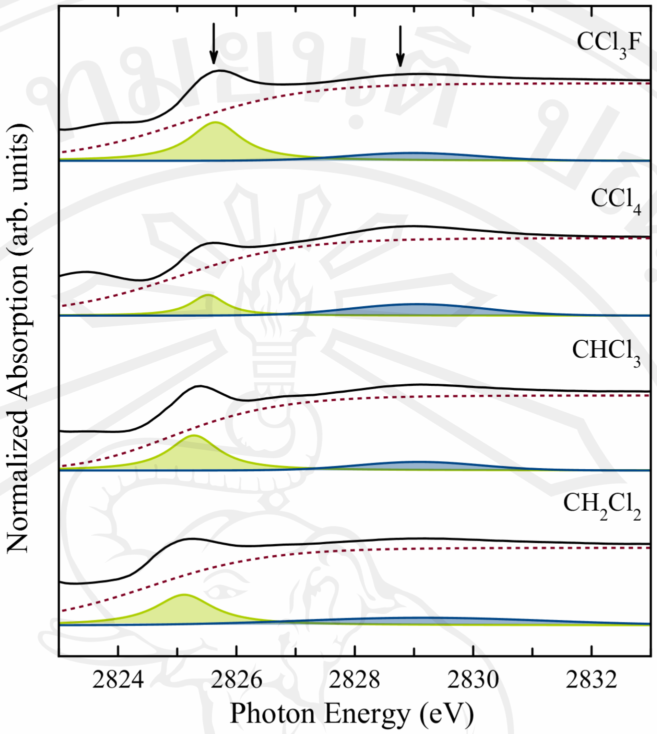

Figure 4.15: The higher energy peak in pre-edge region and multiple-scattering resonance of normalized Cl K-edge spectra of Cl compounds. Deconvolution of XANES spectra made using MagicPlot Pro 2.0.1 is shown under the data.

The ratio of the areas of higher energy peak (C) in pre-edge region and the multiple-scattering resonances peak (D) was determined. By using this method for all chlorine compounds, the results show that selected chlorine compounds can be separated into three groups. These groups are in good agreement with symmetry of molecule structure, which suggests that the symmetry of molecule structure in the sample can be evaluated from the ratio of each peak area.

Table 4.5. The peaks fit of Cl K-Edges of Chlorine compounds.

Sample	Peak C		Peak D		C : D Ratio*
	Position/eV	area	Position/eV	area	
CCl_4	2825.5	0.325	2829.1	1.143	22 : 78
CCl_3F	2825.6	0.742	2829.0	0.280	73 : 27
$CHCl_3$	2825.3	0.673	2829.1	0.286	70 : 30
CH_2Cl_2	2825.1	0.743	2829.2	0.506	59 : 41

* Ratio of the area of peak C : peak D

The results suggested that CCl_4 structure is tetrahedral and also T_d symmetry point group, CCl_3F and $CHCl_3$ structure are same C_{3v} symmetry point group in its group electron state due to the ratio of the areas of the peak C and peak D to be 73:27 and 70:30, respectively. However, the ratio of peak area of CH_2Cl_2 is 59:41, which indicated the molecule structure is C_{2v} symmetry point group.